NDT&E International 139 (2023) 102942

Contents lists available at ScienceDirect

NDT and E International

journal homepage: www.elsevier.com/locate/ndteint

IPSO-VMD based signal feature extraction and internal defect detection of hardwood logs through acoustic impact test

Feng Xu [a,**], Yin Wu [a], Haifeng Lin [a], Yunfei Liu [a,*], Xiping Wang [b], Robert J. Ross [b], Guiyun Tian [c]

[a] *College of Information Science and Technology, Nanjing Forestry University, Nanjing, 210037, PR China*
[b] *USDA Forest Products Laboratory, 1 Gifford Pinchot Drive, Madison, WI, 53726-2398, USA*
[c] *Newcastle University, School of Electrical and Electronic Engineering, Newcastle Upon Tyne, NE1 7RU, Tyne & Wear, UK*

ARTICLE INFO

Keywords:
Hardwood log
Feature extraction
Defect detection
Variational modal decomposition
Improved particle swarm optimization

ABSTRACT

Accurate quality detection of hardwood logs can realize efficient utilization of wood and provide significant benefits to wood enterprises. However, due to the differences in the extraction principle of acoustic parameters and the interaction mechanism between the parameters and wood properties, the quality assessment results of hardwood logs are different to some extent. For this, a method for feature extraction of the acoustic signal and defect detection was proposed based on the improved particle swarm optimization-variational modal decomposition (IPSO-VMD). By analyzing the sparse features of defect signals, the minimum mean envelope entropy was set as the fitness function of IPSO optimized VMD to search for the optimal number pair (L, α). And the search for IPSO was accelerated to acquire the global optimal solution by improving the inertia weight and learning factor of PSO. Then, the effective sub-modes decomposed from the IPSO-VMD were selected based on Hilbert marginal spectrum and energy ratio of sub-band components, and the frequency sub-band distribution and energy rates of the effective modes sifted were used as the characteristic parameters characterized the defect signal to realize the accurate quality detection of hardwood logs. The sawing results of the sample logs showed that the major defect types and priorities in logs were detected with an accuracy of 88.4% and 74.4% respectively based on the IPSO-VMD method, even for which not identifiable by global parameters could be also examined effectively. The effectiveness of the new feature parameters can provide a reliable basis for the accurate quality detection of hardwood logs through fusing the multi-parameter features and constructing the artificial intelligence recognition system in the future.

1. Introduction

Hardwood log is an ideal raw material for producing high value-added wood products because of its rich texture, high aesthetic value, and regenerative nature. In addition, with the rise of large-scale wooden buildings in the world, hardwood logs with high mechanical strength, green and low-carbon and prefabricated forming have also become a potential high-quality material of building structure. Hardwood log usually contains some typical defects of rot, voids, and cracks, and the number and severity of defects vary significantly with origin, species, and even with different parts of the same tree. Early inspection of major internal defects of log can not only save processing costs and improve production efficiency for wood enterprises but also increase the utilization rate of wood to ultimately realize the optimal utilization of wood and maximize profits [1,2].

Acoustic technology has been one of the most popular and useful means in wood detection due to its advantages of low cost, quick and convenient operation, and ease of work on site. Some research has shown that physical or structural damage could have a great influence on the characteristics of acoustic wave propagating in hardwood log, but the correlation between the known acoustic parameters and the hardwood log properties is not significant, and the accuracy in log quality evaluation is far from expectation [3,4]. Using the time-frequency analysis technology, Xu et al. [5,6] extracted some acoustic evaluation parameters such as time centroid, damping ratio and kurtosis, and they reported that the acoustic parameters were better indicators in log

* Corresponding author.
** Corresponding author.
E-mail addresses: fxu@njfu.edu.cn (F. Xu), lyf@njfu.com.cn (Y. Liu).

https://doi.org/10.1016/j.ndteint.2023.102942
Received 12 October 2022; Received in revised form 23 June 2023; Accepted 14 August 2023
Available online 18 August 2023

quality prediction in terms of accuracy in quality grading or internal defects prediction comparing with the acoustic velocity, and which is insusceptible to wood species. Later on this basis, Xu et al. [7] further proposed an approach to assessing internal quality of hardwood log integrated signal separation technology and wavelet based spectral kurtosis. The research indicated that the parameters of kurtosis and spectral kurtosis acquired from defect signals separated could more accurately assess the internal condition of hardwood logs. Even so, owing to the differences in the extraction principle of acoustic parameters and the interaction mechanism between the parameters and wood properties, the evaluation results in hardwood quality were different to some extent. Therefore, it is expected to seek novel acoustic parameters as effective features of the subsequent multi-parameter fusion for constructing the artificial intelligence recognition system to accurately evaluate internal quality in hardwood logs.

The log detection signal is a nonlinear, multi-feature overlapping signal, which causes great difficulty to extract characteristic parameters reflecting wood properties. Trnka et al. [8] studied the propagation characteristics of shock stress waves in wood bars of five tree species, and indicated that the dispersion and attenuation of waves in wood bars could be analyzed in more detail in frequency domain compared with the propagation behavior of waves described in time domain. Lawday and Hodges [9] evaluated the internal condition of ash standing wood combined stress wave technology with a short-time Fourier transform, and they implied the time-frequency spectrum of the acoustic signal was a better assessment index of the decay detection of standing wood. In addition, some studies also pointed out that time-frequency characteristics of acoustic signals seeking from the perspective of signal adaptive decomposition should be a feasible method for defect identification of structure [5,7,10–13].

Variational mode decomposition (VMD) is a new signal processing means with variable scale put forward by Dragomiretskiy and Zosso in 2014 [14], which can decompose a complex signal into a preset scale of amplitude-modulated-frequency- modulated components, effectively suppress mode aliasing, and be appropriate for the feature extraction of non-linear, non-stationary signals. VMD has been gradually applied to pipeline leak detection [15,16], EEG signal classification [17], structure and health monitoring [18], and fault diagnosis [19].

It is necessary to preset the penalty factor α and the number of modes L before a signal is decomposed by VMD. From the VMD theory, the penalty factor α mainly influences the bandwidth of the mode function, while the improper preset number of subcomponents L results in modal aliasing or over-decomposition, which will affect the characteristic representation of the signal. Therefore, the appropriate number pair (L, α) is the key to accurately extracting defect information. At present, some optimization algorithms [20–24] have been used in the optimal mode selection of VMD. The improved particle swarm optimization (IPSO) will be applied to optimize the number pair (L, α) of VMD in the present study given the characteristics of IPSO such as fast convergence, less parameter setting, and easy implementation [25,26].

Based on defect signal separation in the literature [7], a method of feature parameter extraction and defect identification was proposed based on the IPSO-VMD in this study. By analyzing the sparse characteristics of defect signals, the minimum mean envelope entropy (MMEE) was set as the fitness function of IPSO optimized the VMD to realize the search of the optimal number pair (L, α). For accelerating the search for the PSO algorithm to reach the global optimal solution, the inertia weight and learning factor of PSO were improved. Then, the effective modes of representing the original signal were selected based on Hilbert marginal spectrum and frequency band (FB) energy ratio (ER). Finally, the FB distribution and ER of each effective sub-mode were determined as the characterization parameters of type and primary-secondary of the main defects in hardwood logs to achieve a relatively accurate evaluation in the internal quality of hardwood logs.

2. Variational modal decomposition algorithm

Variational mode decomposition (VMD) decomposes an input signal into a series of modal components with sparsity properties through iteratively searching for the optimal solutions of the variational model [14]. Each sub-component is called band-limited intrinsic mode function (BIMF), which is a limited bandwidth signal centered on frequency ω, i.e.

$$u_k(t) = A_k(t)\cos[\varphi_k(t)] \tag{1}$$

where $u_k(t)$ is the k-th mode, $A_k(t)$ is the instantaneous amplitude, $\varphi_k(t)$ is a non-decreasing phase function, i.e. $\varphi_k^{'}(t) \geq 0$, and the change of $A_k(t)$ and instantaneous angular frequency $\omega_k(t) = \varphi_k^{'}(t)$ is much less than that of $\varphi_k(t)$.

To solve each BIMF and estimate its bandwidth, VMD introduces a constrained variational model as shown in Eq. (2):

$$\begin{cases} \min\limits_{\{u_k\},\{\omega_k\}} \left\{ \sum\limits_{L} \left\| \partial_t [(\delta(t) + \mathrm{j}/\pi t) * u_k(t)] \exp(-\mathrm{j}\omega_k t) \right\|_2^2 \right\} \\ \qquad s.t. \quad \sum\limits_{L} u_k = x(t) \end{cases} \tag{2}$$

where ω_k is the center frequency of u_k, L is the number of the BIMFs, ∂_t is the partial derivative with respect to time, δ is the Dirac function, the symbols $\|\bullet\|$ and $*$ represent the norm and convolution operation respectively, and x is the original signal.

For solving the variational problem, the quadratic penalty factor α and the Lagrange multiplier λ are introduced to transform Eq. (2) into the augmented Lagrange equation shown in Eq. (3),

$$\mathscr{L}(\{u_k\},\{\omega_k\},\lambda) = \alpha \sum_{k=1}^{L} \left\| \partial_t [(\delta(t) + \mathrm{j}/\pi t) * u_k(t)] \exp(-\mathrm{j}\omega_k t) \right\|_2^2$$

$$+ \left\| x(t) - \sum_{k=1}^{L} u_k(t) \right\|_2^2 + \left\langle \lambda(t), x(t) - \sum_{k=1}^{L} u_k(t) \right\rangle \tag{3}$$

where, the symbol $<\bullet>$ represents inner product. The parameter α can reduce the effect of Gaussian noise to ensure the fidelity of signal reconstruction, and λ can enforce strict constraints of the model [14].

The minimization of the L^2-norm of the gradient of Eq. (2) can be transformed into seeking the saddle point of Eq. (3) using the alternating direction method of multipliers (ADMM). The problem can be solved in the frequency domain by using the Plancherel Fourier isometry of the norm and Hermitian symmetry, i.e. the preset number of BIMF can be obtained by inputting the currently optimized solution into the ADMM algorithm and updating $\widehat{u}_k^{n+1}$, ω_k^{n+1}, and $\widehat{\lambda}^{n+1}$ alternately according to Eqs. (4)–(6) until the termination condition of Eq. (7) is satisfied.

$$\widehat{u}_k^{n+1}(\omega) = \frac{\widehat{x}(\omega) - \sum\limits_{i=1, i<k}^{L} \widehat{u}_i^{n+1}(\omega) - \sum\limits_{i>k}^{L} \widehat{u}_i^{n}(\omega) + \widehat{\lambda}^{n}(\omega)/2}{1 + 2\alpha(\omega - \omega_k^n)^2} \tag{4}$$

$$\omega_k^{n+1} = \int_0^\infty \omega \left| \widehat{u}_k^{n+1}(\omega) \right|^2 \mathrm{d}\omega \Big/ \int_0^\infty \left| \widehat{u}_k^{n+1}(\omega) \right|^2 \mathrm{d}\omega \tag{5}$$

$$\widehat{\lambda}^{n+1}(\omega) = \widehat{\lambda}^{n}(\omega) + \gamma \left[\widehat{x}(\omega) - \sum_{k=1}^{L} \widehat{u}_k^{n+1}(\omega) \right] \tag{6}$$

$$\sum_k \left\| \widehat{u}_k^{n+1} - \widehat{u}_k^{n} \right\|_2^2 \Big/ \left\| \widehat{u}_k^{n} \right\|_2^2 < e \tag{7}$$

where $\widehat{u}_k^{n+1}(\omega)$ is the output from Wiener filtering of residual $\widehat{x}(\omega) - \sum_{i=1, i\neq k}^{L} \widehat{u}_i^{n}(\omega)$, γ is the noise tolerance, and e is the convergence termination condition.

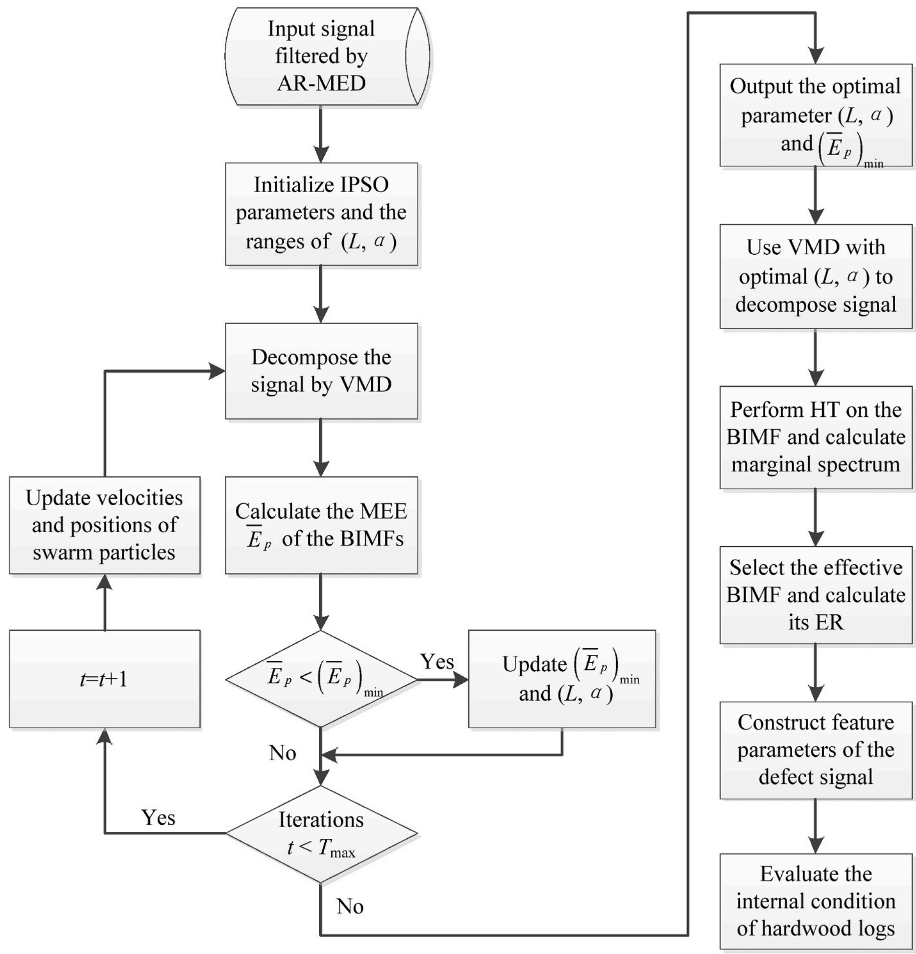

Fig. 1. Flow chart of quality evaluation of hardwood logs based on IPSO-VMD.

3. Defect recognition based on the IPSO-VMD algorithm

3.1. IPSO-optimized VMD method

Particle swarm optimization (PSO) is a population-intelligent stochastic algorithm proposed by Kennedy and Eberhart inspired by the foraging behavior of birds [25,26]. Each particle in PSO searches for the optimal solution to the optimization problem in the search space by constantly updating the spatial posture (migration speed and position). PSO algorithm has been widely applied in solving nonlinear problems in recent years because of its fast and accurate convergence and high efficiency in solving global optimal solutions.

The decomposition results of VMD highly depend on the preset number pair (L, α). Improper number pair setting will seriously affect the accuracy of feature extraction of defect signals and lead to the misjudgment of hardwood log quality. Therefore, it is particularly important to introduce a two-dimensional particle swarm to optimize simultaneously the number pair of VMD. The combination parameter (L, α) is regarded as a two-dimensional swarm particle, and its initial and updating velocity and position satisfy the iterative relation of Eqs. (8) and (9) for searching for a better posture, until the optimal solution is reached.

$$\begin{bmatrix} v_{L_i}^{n+1} \\ v_{\alpha_i}^{n+1} \end{bmatrix} = w \begin{bmatrix} v_{L_i}^{n} \\ v_{\alpha_i}^{n} \end{bmatrix} + l_1 r_1 \left(\begin{bmatrix} p_{L_i}^{n} \\ p_{\alpha_i}^{n} \end{bmatrix} - \begin{bmatrix} x_{L_i}^{n} \\ x_{\alpha_i}^{n} \end{bmatrix} \right) + l_2 r_2 \left(\begin{bmatrix} g_{L_i}^{n} \\ g_{\alpha_i}^{n} \end{bmatrix} - \begin{bmatrix} x_{L_i}^{n} \\ x_{\alpha_i}^{n} \end{bmatrix} \right) \tag{8}$$

$$\begin{bmatrix} x_{L_i}^{n+1} \\ x_{\alpha_i}^{n+1} \end{bmatrix} = \begin{bmatrix} x_{L_i}^{n} \\ x_{\alpha_i}^{n} \end{bmatrix} + \begin{bmatrix} v_{L_i}^{n+1} \\ v_{\alpha_i}^{n+1} \end{bmatrix} \tag{9}$$

where w is inertia weight balancing local and global search ability; l_1 and l_2 are learning factors, which represent a particle self-cognition and swarm learning ability respectively; r_1 and r_2 are random numbers between 0 and 1. $v_{\bullet i}^{n}$, $x_{\bullet i}^{n}$ and $p_{\bullet i}^{n}$ is the current velocity, position, local optimal value of the i-th particle in the n-th iteration respectively; $g_{\bullet i}^{n}$ is the global extreme value of swarm particles in the n-th iteration.

According to Eq. (8), the performance of PSO mainly relies on the control parameters w, l_1, and l_2. Thus, appropriate number pair configuration can accelerate the convergence of the algorithm to achieve the global optimal value. In the study, an improved PSO (IPSO) algorithm was proposed to realize a fast optimization process of number pair (L, α) for VMD by adjusting w as nonlinear decreasing inertia weight as shown in Eq. (10), l_1 and l_2 as synchronous learning weights as shown in Eq. (11).

$$w = w_{max} - (w_{max} - w_{min})(t/T_{max})^n \tag{10}$$

$$l_1 = l_2 = l_{max} - (l_{max} - l_{min}) \times t \,/\, T_{max} \tag{11}$$

where w_{max}, w_{min}, l_{max} and l_{min} are the maximum and minimum inertia weight and learning factor respectively; t and T_{max} are the current and maximum iteration number respectively; n is the nonlinear adjustment factor, which ensures the higher accuracy by iterative fine-tuning in the later period of the search process.

In the procedure of IPSO optimizing the number pair (L, α) of VMD, selecting the fitness function is critical for the final optimization result. When the cross-section of a hardwood log is subjected to unit longitudinal impact, the excited vibration signal presents the internal condition of the log. If a log is in soundness, the response signal is the

Table 1
Species, physical parameters and defect types of the hardwood logs.

Log No.	Species	Length/(m)	Diameter (D)/(cm)						MC (%)	Defects observed
			D_L^a		D_S^b		Average			
							D_L	D_S		
1	Black cherry	2.44	45.4	39.1	38.0	38.1	42.2	38.1	48.4	Solid, end crack
2	Red oak	2.54	54.0	53.3	40.6	38.7	53.7	39.7	39.7	Rot, void, crack, hole
3	White oak	2.62	38.6	38.1	38.4	28.6	38.3	33.5	80.8	Void, crack, decay, ring shake (broken into pieces), hole.
4	Red oak	2.49	34.1	25.6	23.2	20.6	29.9	21.9	61.6	Void, decay, crack (broken into pieces)
5	Black cherry	2.62	48.6	43.2	44.3	38.6	45.9	41.4	58.3	Crack, void, decay
6	White oak	2.48	38.1	35.9	33.0	33.0	37.0	33.0	31.3	Void, decay, knots
7	Red oak	2.67	61.9	59.2	51.8	51.4	60.6	51.6	75.9	Void, decay, ring shake
8	Cottonwood	2.60	36.2	35.6	35.7	35.6	35.9	35.6	95.6	Ring shake, decay
9	Red oak	2.53	51.4	45.7	43.5	41.0	48.6	42.2	86.0	Void, decay, hole
10	White oak	2.46	31.0	30.6	26.0	23.8	30.8	24.9	52.5	Void, decay, split,
11	White oak	2.55	55.7	50.8	38.1	37.8	53.3	37.9	77.4	Void, crack
12	White oak	2.34	38.9	35.6	31.1	30.5	37.2	30.8	46.6	Extensive check, rot, decay, end crack
13	Cottonwood	2.44	33.0	31.4	31.4	28.1	32.2	29.8	76.8	Split, surfaces decay, heartwood decay, bow
14	Red oak	2.59	38.4	38.1	35.9	35.6	38.3	35.7	68.8	Void, decay, ring shake, radial crack, knots
15	Red oak	2.64	44.0	39.2	45.5	43.5	41.6	44.5	70.3	Split, internal crack (broken pieces), end crack, void, decay

[a, b] D_L and D_S are for the diameters of large end and small end, respectively.

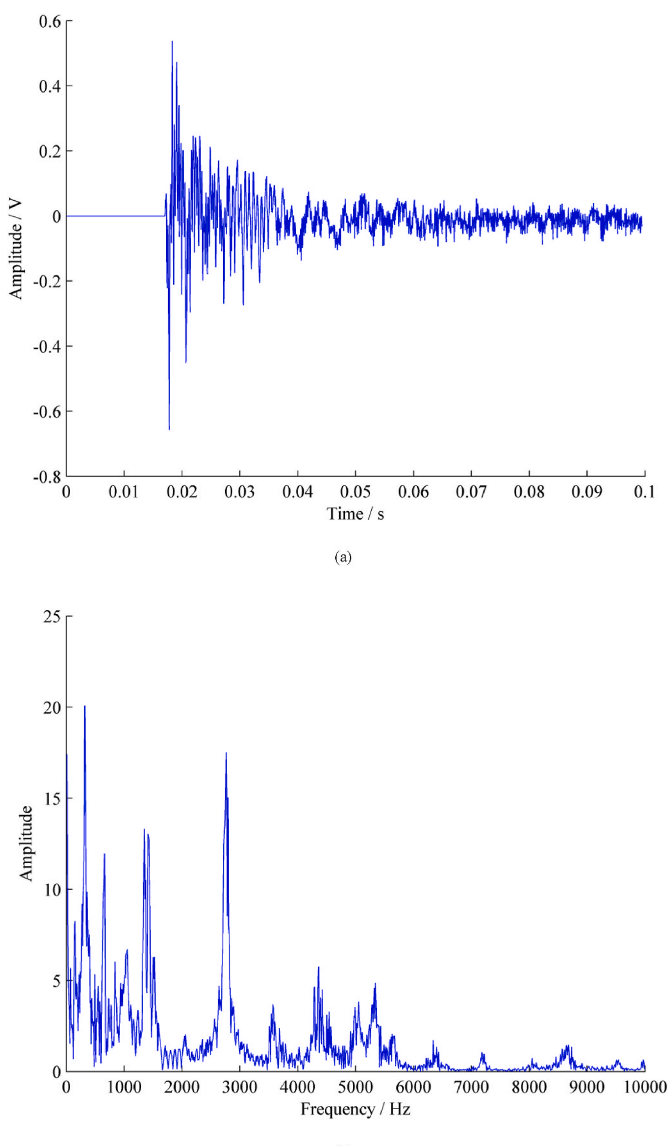

Fig. 2. Acoustic response signal of log no.5. (a) Time history of the response signal filtered by AR-MED method. (b) Frequency spectrum of the response signal.

superposition of infinite many principal modes with different natural frequencies according to the vibration theory, and which is non-sparse in the time domain. However, if there exist internal defects in a log, the response signal will inevitably show strong sparsity properties due to mutation, distortion, or attenuation components induced by the defects. Some research shows that the signal envelope entropy can correctly reveal the sparse characteristics of the signal, that is, the stronger sparsity of the signal, the smaller envelope entropy value, and vice versa [7,19]. As a result, the envelope entropy E_{pk} of each BIMF u_k decomposed from VMD can be used as the fitness function of IPSO optimizing VMD, and its definition is shown in Eq. (12)

$$\begin{cases} E_{pk} = -\sum_{i=1}^{N} p_{ki} \log_2(p_{ki}) \\ p_{ki} = a_{ki} \Big/ \sum_{i=1}^{N} a_{ki} \end{cases} \tag{12}$$

where p_{ki} is the probability density function of u_k, and N is the length of the signal. a_{ki} is the envelope amplitude of u_k processed by Hilbert transform.

The optimal number pair (L, α) of VMD can be acquired by searching for the minimum mean envelope entropy (MMEE) as shown in Eq. (13).

$$(L, \alpha) = \arg\min_{(x_L, x_\alpha)} \left\{ \overline{E}_p = \sum_{k=1}^{L} E_{pk} \Big/ L \right\} \tag{13}$$

where $\overline{E}_p$ is the mean envelope entropy (MEE).

3.2. Identification of internal defects in hardwood log

The defect identification flowchart based on IPSO-VMD is shown in Fig. 1. The general steps are as follows.

(1) Set a range of number pair (L, α) of VMD to be optimized and the initial values of IPSO.
(2) Apply VMD to decompose the input defect signal filtered by AR-MED. Then $\overline{E}_p$ of all modes is calculated according to Eqs. (12) and (13) and saved as the initial value $(\overline{E}_p)_{\min}$. Meanwhile the number pair (L, α) corresponding to $(\overline{E}_p)_{\min}$ is also saved as the initial optimal position of the particle swarm.
(3) Update speeds and positions of the current population particles according to Eqs. (8) and (9), and perform VMD on the signal again and calculate the $\overline{E}_p$.

Table 2
The initial parameters of IPSO and the ranges of parameter pair (L, α) of VMD.

Category	Scale of swarm	Iteration number	Inertia weight/w		Learning factors/l		Migration velocity/v				The ranges of (L, α)			
	Scal	T_{max}	w_{max}	w_{min}	l_{max}	l_{min}	v_{Lmax}	v_{Lmin}	$v_{\alpha max}$	$v_{\alpha mix}$	L_{max}	L_{min}	α_{max}	α_{min}
Value	100	30	0.9	0.4	2.1	0.8	50	−50	2	−2	11	2	3000	500

(4) After each iteration, the current $\bar{E}_p$ and $(\bar{E}_p)_{min}$ are compared. If $\bar{E}_p < (\bar{E}_p)_{min}$, $(\bar{E}_p)_{min}$ and number pair (L, α) corresponding to the $(\bar{E}_p)_{min}$ are updated; otherwise, original values remain unchanged.
(5) Repeat steps (3) to (4) until the end of the iteration, and acquire the $(\bar{E}_p)_{min}$ of the particle swarm and the optimal number pair (L, α).
(6) Perform VMD with optimal number pair (L, α) on the input signal to obtain the BIMF containing the local characteristics of the signal in time-field and frequency-field.
(7) Perform Hilbert transform on each BIMF to obtain its marginal spectrum. And the effective BIMF was selected by eliminating BIMF with smaller spectral amplitude to reduce the dimension of feature parameters for simplifying the difficulty of analysis.

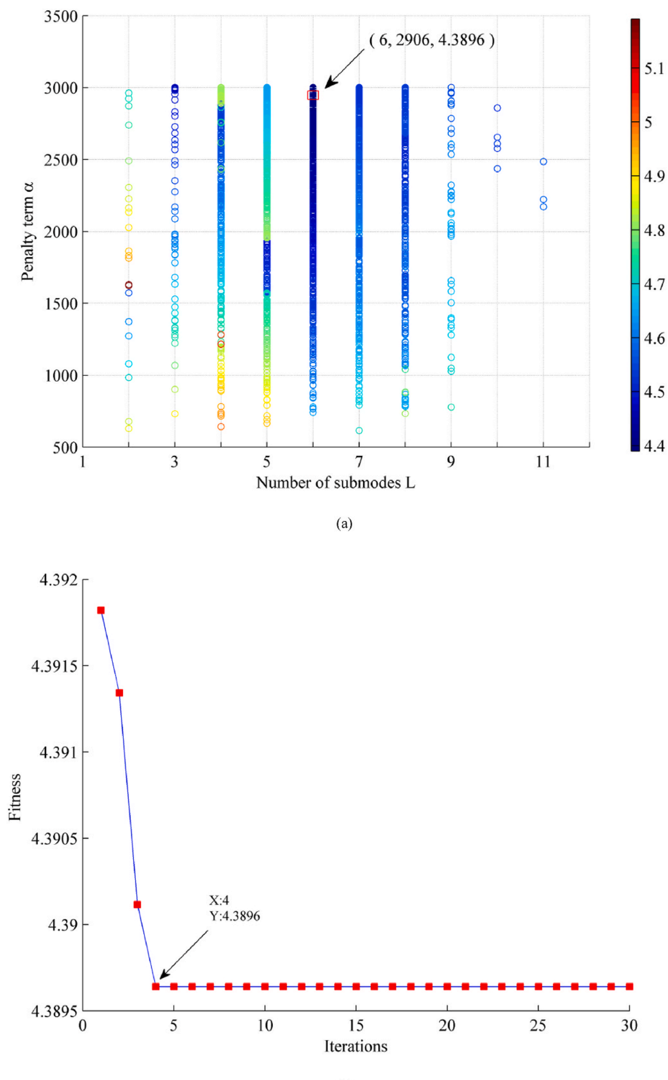

Fig. 3. The IPSO optimization process for VMD parameters. (a) The distribution of MEE with different number pair (L, α). (b) Evolution curve of fitness function MEE during the iteration process.

(8) Calculate the ER of effective BIMF respectively according to Eq. (14), and establish the acoustic feature parameters of log based on ER and FB distribution of the modes for identification of internal defect types and damage degrees of hardwood logs.

$$E_{u_k} = \sum_{i}^{n} (u_k(i))^2 \Bigg/ \sum_{k=1}^{L} \left(\sum_{i}^{n} (u_k(i))^2 \right) \times 100\% \tag{14}$$

4. Materials and methods

Fifteen log samples of four hardwood species were provided by a local wood-working enterprise in Madison, Wisconsin, USA for this study. These samples consisted of both sound and unsound logs. The flawed logs had a wide variety of internal defects deteriorated in different levels. Upon delivery to the USDA Forest Service, Forest Products Laboratory, the logs were placed on the ground inside a building and each log was assigned a log number before testing. Acoustic impact tests were performed on these samples on the ground in longitudinal and radial directions respectively. The purpose of the longitudinal test was to obtain an acoustic vibration signal collected by a data acquisition card linked to a laptop for quality detection of logs (sampling frequency of 20 kHz and sampling length of 2000 points). The stress wave transmission time measured in the radial direction was applied to evaluate the physical conditions of each log at various test locations to select the dissecting locations for further determining the internal defects and distribution in the logs. The measurement started from the large end 30 cm from the cross-section of each log and stepped in every 30 cm until the whole log was tested. The selection principle of log samples, measurement of log dimension and moisture content, testing environment and processes are detailed in Xu et al. [6]. For the convenience of analysis, the log species, physical parameters, and internal conditions of the logs are listed in Table 1.

5. Results and discussion

The acoustic response signal acquired from a log can be described as the convolution between the combined signal of harmonic resonance, defect components, and background noise and the response function of the transmission path. To accurately extract the characteristics of defect signals, this study applied the AR-MED method proposed in the literature [7] to obtain the defect components separated from the acoustic signal (which is not the focus of this paper and will not repeat here). And then defect signals were decomposed using the IPSO-VMD for extracting the feature vectors of effective sub-modes to achieve an accurate assessment of the internal condition of logs.

5.1. Effective modal selection based on IPSO-VMD and marginal spectrum

To illustrate the selection process of effective sub-modes, this paper took the response signal of log no.5 as an example. The time domain signal and its spectrum of log no.5 are shown in Fig. 2. Although the global feature parameters of the acoustic signal can reflect the internal damage conditions of a log to some extent, it is difficult to obtain the features of log quality distribution through single time- or frequency-domain analysis. As a result, it is impossible to assess the types and priorities of internal defects of a log [6,7]. As can be seen from the spectrum distribution shown in Fig. 2 (b), the signal components are

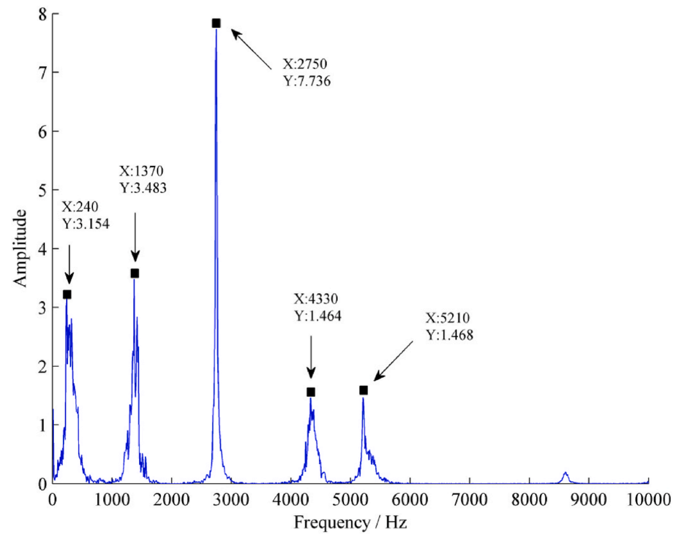

Fig. 4. Marginal spectrum of all modes from log no.5 signal decomposed by IPSO-VMD, which was applied for selection of the effect modes preliminarily.

abundant from low to high frequencies, especially the amplitude of the FB below 3 kHz is significantly higher than those of the other FBs. The IPSO-VMD method was used to decompose the signal, and the initialization parameters of the algorithm were listed in Table 2. The initial values of the number pair (L, α) and the particle migration velocity v are randomly distributed but need to meet the constraint of extreme values respectively in Table 2. Fig. 3 (a) is the 2-D mesh of the MMEE search process for different number pairs (L, α). As shown in the red box in the figure, the MMEE and the optimal number pair corresponding to MMEE are $(\bar{E}_p)_{\min} = 4.390$ and (L, α)=(6, 2906) respectively, which indicates the signal can be decomposed into 6 sub-modes and the corresponding MEE is the smallest. It can be seen from the optimization process in Fig. 3 (a) that the updating speeds of α and L in the IPSO algorithm are variational, thus the particle swarm moves toward the direction of MMEE with different step sizes of v_α and v_L. This property highly reduces the times of repeated cross-iterations and significantly improves the speed of optimization. In addition, the evolution curve of MME shown in Fig. 3 (b) indicates search process of the optimal value is accelerated obviously for the introduction of the nonlinear decreasing inertia weight and synchronous learning factor, and the optimal solution is achieved by only four iterations.

It is important to select the effective sub-modes from all modes decomposed by IPSO-VMD for simplifying the analysis. From the signal analysis theory, it is known the frequency amplitude of a certain point in the Fourier spectrum only represents the trigonometric component with this frequency existing in a signal, while the actual components of the non-stationary signal cannot be accurately expressed. However, Hilbert marginal spectrum characterizes the cumulative amplitude distribution of each frequency point in the statistical sense, namely if there exists the energy of a certain frequency in a signal, it implies the vibration signal with this frequency must appear. Therefore, the marginal spectrum can be regarded as a kind of weighted joint distribution of amplitude-frequency- time, that is, the amplitude of the marginal spectrum can be used to select the effective modes of a decomposed signal.

The marginal spectrum of the BIMFs u_1-u_6 decomposed by IPSO-VMD was obtained through the Hilbert transform. As shown in Fig. 4, the marginal spectrum was closely related to the Fourier spectrum shown in Fig. 2 (b), but the former eliminated the possible pseudo-harmonic frequency components in the Fourier spectrum. In Fig. 4, the center frequencies of the first five modes were 240 Hz, 1370 Hz, 2750 Hz, 4330 Hz, and 5210 Hz respectively, with corresponding amplitudes of 3.154, 3.483, 7.736, 1.464, and 1.468, which were much higher than that of the sixth mode. The result indicated that the occurrence probability of vibration signals with the above frequencies was much higher than that of the last one. Therefore, the first five BIMFs could be preliminarily determined as the effective modes of the signal. The time-domain waveforms and Fourier spectrums of u_1-u_5 were shown in Fig. 5. Obviously, the signal had been decomposed, and no mode aliasing phenomenon.

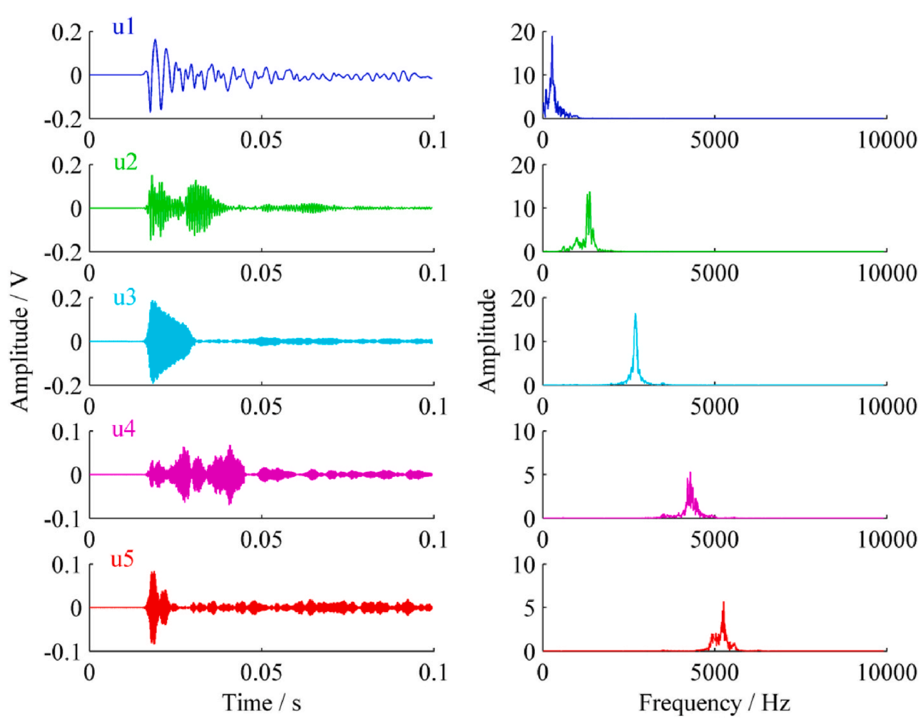

Fig. 5. The effective BIMFs sifted by the marginal spectrum and the corresponding frequency spectra.

Table 3
The corresponding relation between distribution of FBs and type of defects.

Distribution of FBs (Hz)	Type of defects	Distribution of FBs (Hz)	Type of defects
150–750	Void	1950–2550	Split, crack, ring shake
750–1350	Rot or severe decay	2550–2850	End check
1350–1650	Intermediate decay	Above 2850	Solid
1650–1950	Incipient decay		

5.2. Extraction of characteristic parameters based on the ER of BIMF

In general, the larger the energy of a sub-mode is, the more significant the useful characteristic information it contains. Therefore, the ratio of the energy of each sub-mode to the total energy of a signal can be used as a means to further determine the effective mode of the signal. Considering that the BIMF is a narrowband signal, and referring to the research results of reference [7], the ER of each sub-mode can be regarded as the ER of a narrowband signal centered on its marginal spectrum and with a bandwidth of 300 Hz. For example, the center frequency of u_3 mode is of 2750 Hz, its ER can be considered as that of the narrowband component with a bandwidth of 2600–2900 Hz to the total energy of the signal. So, the ERs of u_1-u_5 modes of log no.5 could be acquired according to Eq. (14), which were 34.6%, 24.9%, 32.2%, 3.7%, and 3.9% respectively. In this paper, 5% of the total energy is taken as the threshold for selecting the effective modal, that is, if the ER of a mode is greater than 5%, the mode can be considered as a signal component caused by material characteristics (such as defects), while if one less than 5%, the mode be related to noise and ignored. As a result, for the signal from log no.5, its sub-modes u_1-u_3 were determined as the final effective modes, and their ERs were used as the characterization parameters of type and priority of internal defects in logs.

Xu et al. [7] indicate that the higher the certain sub-band energy is, the greater the proportion of a material component associating with the sub-band in a log occupies. Furthermore, some studies show that if the internal defects of a log are mainly voids or decay, the frequencies of an acoustic wave propagating in the log are relatively low [27–29], but if dominant defects in a log are cracks or splits, the acoustic signal contains much of high-frequency components [30]. Therefore, it is inferred that if the ER of the low FB of a signal is relatively high, there will be some

(a) (b) (c) (d) (e) (f) (g) (h) (i) (j) (k) (l) (m) (n) (o)

Fig. 6. Defects located in the end face and dissected cross-section of 15 logs. (a) End checks in the log no.1. (b) Rot, void, crack, etc. in the log no.2. (c) Void, crack, decay, ring shake, etc. in the log no.3. (d) Void, decay and crack in the log no.4. (e) Crack, void and decay in the log no.5. (f) Void and decay in the log no.6. (g) Void, decay and ring shake in the log no.7. (h) Ring shake and decay in the log no.8. (i) Void and decay in the log no.9. (j) Void, decay and split in the log no.10. (k) Void and crack in the log no.11. (l) Extensive check, rot, decay and end crack in the log no.12. (m) Split, surfaces decay and heartwood decay in the log no.13. (n) Void, decay, ring shake and radial crack in the log no.14. (o) Split, internal crack (broken pieces), end crack, void and decay in the log no.15.

Table 4
Acoustic feature parameters of the response signals and predicted defects of hardwood logs.

Log No.	Energy ratio in FBs (%)												Prediction of defect type
	150- 750 (Hz)		750- 1950 (Hz)				1950- 2550 (Hz)		2550- 2850 (Hz)	2850-3750 (Hz)			
	150-450	450-750	750-1050	1050–1350	1350–1650	1650–1950	1950–2250	2250–2550		2850–3150	3150–3450	3450–3750	
1	–	–	–	–	–	–	–	–	18.6	38.5	35.4	–	Solid but end checks
2	–	14.2	5.5	–	29.1	30.3	18.9	–	–	–	–	–	Incipient decay, rot, void
3	21.5	–	16.7	–	–	–	22.2	35.0	–	–	–	–	Ring shake, crack, void, rot
4	9.9	–	32.4	–	–	30.3	–	18.5	7.9	–	–	–	Rot, incipient decay, crack, void, end checks
5	34.6	–	–	–	24.9	–	–	–	32.2	–	–	–	Void, end checks, intermediate decay
6	66.9	–	–	–	–	33.1	–	–	–	–	–	–	Void, incipient decay
7	–	40.5	–	–	51.5	–	6.6	–	–	–	–	–	Intermediate decay, void, crack
8	–	–	17.8	–	–	–	–	82.2	–	–	–	–	Ring shake, rot
9	–	19.4	–	43.5	37.0	–	–	–	–	–	–	–	Rot, Intermediate decay, void
10	44.8	–	45.4	–	–	–	9.9	–	–	–	–	–	Rot, void, split
11	51.0	6.9	–	–	–	–	–	5.1	–	–	–	32.0	Void, crack
12	–	–	43.6	–	–	–	56.4	–	–	–	–	–	Crack, rot
13	–	–	–	–	12.8	–	–	87.2	–	–	–	–	Split, intermediate decay
14	–	23.7	–	54.9	–	–	–	19	–	–	–	–	Rot, void, ring shake
15	–	20.2	17.2	–	17.8	–	42.8	–	–	–	–	–	Split, crack, void, rot, intermediate decay

defects such as voids or decay in a log; On the contrary, if the energy of the high FB is dominant, cracks, splits or end shakes will appear in the log. Combined with the analysis of literature [7], the corresponding relationship between the main defects of a log and FBs of a signal as shown in Table 3 could be determined.

Given the distribution of FBs and ER of effective modes u_1-u_3, it could be speculated from Table 3 that there should be some defects such as void, intermediate decay, and end checks in log no.5, and the void was the most significant among these defects. Checking the internal condition of the log (as shown in Fig. 6 (a)), it was found that all three were the main defects, and the decay was relatively weak among them. The prediction results were basically consistent with reality. Certainly, other defects, such as knots, were also found in the log, but they were significantly smaller and could be ignored compared with the influence of main defects on log quality. The detection result of log no.5 showed that the corresponding relationship between the distribution of FBs and defect types in Table 3 was correct, and ER of each effective mode basically reflected the damage degree and priority of internal defects.

According to the above method, the distribution of sub-bands and their ERs of all 15 hardwood logs were extracted and listed in Table 4 along with predicted defects of which the priorities had been sorted according to the ERs.

5.3. ER-based defect identification of log

The main sub-modes u_9-u_{11} of log no.1 were located in FB of 2550–3450 Hz, with ERs of 18.6%, 38.5%, and 35.4%, respectively. According to the corresponding relationship in Table 3, there should be no other defects inside of the log apart from end checks, which was confirmed by observing the actual sawing condition (Fig. 6 (b)). The sum of energy of the effective modes of log no.2 accounted for about 98% of the total signal energy, and energy of 450–750 Hz, 1350–1650 Hz, 1650–1950 Hz, and 1950–2250 Hz accounted for 14.2%, 29.1%, 30.3%, and 18.9% respectively. In addition, the energy of the mode u_2 of 750–1050 Hz, although relatively weak compared with other effective modes, also reached 5.5% of the total energy. It could be deduced from Table 3 that there existed some defects of decay, crack, and void in the log and the decay was the most severe one, as evidenced by examining the sawing results (Fig. 6 (c)). The ERs of effective modes of log no.3 were relatively balanced and ranged from 16.7 to 35.0%, indicating that there existed multiple defects in the log and which were all significant. The good consistency between the predicted defects and the actual dissecting results (Fig. 6 (d)) further proved the validity of the corresponding relationship between FB distribution and defect types in Table 3. For log no.4, there was a relatively wide FB distribution of effective modes, ranging from 150 to 2850 Hz, with high ERs. Of which the mode u_2 located at 2550–2850 Hz had the lowest ER of 7.9%, and the highest was u_5 mode situated at 750–1050 Hz, with an ER of 32.4%.The ER distribution of FBs showed that there would exist a series of obvious defects, such as void, rot, incipient decay, crack, end check, etc., in the log. Inspection of the actual cross-sections cut open in the log demonstrated that these defects were clearly visible (Fig. 6 (e)).

A similar analysis could be made for the remaining logs in Table 4 (defects distribution of the logs were shown in Fig. 6 accordingly), no more tautology here due to limited space. By comparing Table 4 with Tables 1 and it could be found that the main defects predicted in most of the logs were consistent with the actual observation, except for some minor defects without prediction and a minor difference in the priority of partial defects. That is, there are 49 defects of all types (including minor defects) in the 15 logs, 43 of which are major defects. 38 major defects were successfully identified, with an accuracy of 88.4%. Even for all of the defects, the prediction accuracy was also about 77.6%. In addition, the prediction accuracy of the primary and secondary main defects reached 74.4%. The analysis results further verified the effectiveness of the proposed method in the quality evaluation of hardwood logs.

The previous study results on log no.8 should be noted. In previous research, Xu et al. [6,7] indicated that the log no.8 should be a high-quality sound wood without defects inferred from the global parameters of the acoustic signal, but obvious ring shakes and some moderate or incipient decay were found to exist in the log during the actual sawing process (Fig. 6 (h)). Examined the distribution of effective modes of log no.8 listed in Tables 4 and it was evidenced that the FBs of 750–1050 Hz and 2250–2550 Hz and the corresponding ER of 17.8% and 82.2% accurately predicted the existence of these two defects in the log, and the primary and secondary of defects was consistent with the actual detection results. The research results showed that the IPSO-VMD based method could effectively ascertain internal defects that could not be detected even by global parameters.

To compare the running speed of the IPSO-VMD method with the spectral kurtosis method proposed in Ref. [7], both were executed in MATLAB installed on the same laptop. The computer had an Intel Core i5-4210u 2.4 G CPU and 4.0 G RAM. It could be observed that the time consumption of the IPSO-VMD is between 10 and 20 min, with an average of 16 min. The time consumption mainly depends on the level of signal decomposition (complexity of signal) and the population size. Wavelet-based spectral kurtosis method takes much less time, with a mean time of about 5 min. However, human intervention in the early stage of the method is neglected, such as the selection of the optimal wavelet base, which requires rich working experience and consumes a lot of time. So, the IPSO-VMD is simpler to implement though it is not dominant in terms of computational speed than the latter.

In short, compared with the spectral kurtosis method, although the representation of the characteristic components (FBs) of the signal caused by defects was not as sensitive as the latter, the energies of the effective sub-modes were more concentrated in certain sub-bands and easier to identify the types and priorities of major defects. In addition, compared with the literature [7], expect for the different feature sub-bands corresponding to voids, the characteristic intervals corresponding to other main defects basically overlapped but were slightly lower in frequencies, which could be caused by the different interaction mechanisms between signal characteristic parameters and wood properties. Taking void as an example, due to a longer path propagating in a log, the energy attenuation of the acoustic wave was larger, which resulted in the FBs represented by ERs being lower; while the spectral kurtosis as the fourth-order statistics reflecting the mutation of signal, whose values increased inevitably in the high FBs caused by void. As a result, there must be certain differences in the analysis results when the two characteristic parameters were used to assess the internal quality of logs. But if the common features of the two could be integrated, the prediction accuracy in log quality should be improvable.

6. Conclusions

Due to the variable natural properties and various defect types of hardwood logs, the acoustic detection signals caused are complicated and overlapped with the characteristic spectrum, which increases the difficulty of internal quality assessment of logs. In this study, a signal feature extraction method based on IPSO-VMD was proposed and a selection means of effective sub-modes was determined. The distribution of FBs and ERs of modes were extracted as characteristic parameters of the main defects to realize the evaluation of the internal quality of hardwood logs.

The research results showed that the VMD could decompose the log defect signal into a series of sub-modes with sparse properties, and the effective sub-modes contained the transient characteristics caused by the main defects. The MMEE related to the sparse features of the sub-modes as the fitness function of IPSO could realize the fast and effective search for the optimal number pair (L, α) of VMD, and improve the adaptation of VMD for the decomposition of non-stationary acoustic vibration signals.

Hilbert marginal spectrum combined with ER of modes could achieve the selection of effective sub-modes decomposed by VMD. And taking the FBs and ERs of the effective sub-modes as the feature parameters, the types and the priorities of major defects of logs could be relatively accurately identified with the accuracy of 88.4% and 77.4% respectively. The IPSO-VMD based method could effectively identify internal defects of logs that could not be detected by global parameters of the acoustic signal.

Although the research results indicated an effective and relatively accurate means of combining the impact testing technology with the advanced IPSO-VMD method to predict types and priorities of internal main defects in the hardwood logs, a production trial with a larger sample size is need to further validate the effectiveness of the acoustic parameters. And so, the internal conditions of hardwood logs could be detected accurately by fusing the multi-parameter features and constructing the artificial intelligence recognition system in the future.

CRediT authorship contribution statement

Feng Xu: Conceptualization, Methodology, Software, Formal analysis, Investigation, Writing – original draft, Writing – review & editing. **Yin Wu:** Data curation, Investigation. **Haifeng Lin:** Formal analysis, Data curation. **Yunfei Liu:** Conceptualization, Methodology, Supervision, Funding acquisition, Review & editing. **Xiping Wang:** Conceptualization, Methodology. **Robert J. Ross:** Conceptualization, Methodology. **Guiyun Tian:** Review & editing.

Declaration of competing interest

The authors declare that they have no known competing financial interests or personal relationships that could have appeared to influence the work reported in this paper.

Data availability

Data will be made available on request.

Acknowledgments

This study was supported by National Natural Science Foundation of China, China (grant no.32171788) and; Key Research and Development Project of Jiangsu Province, China (grant no. BE2021716).

References

[1] Edlund J, Lindström H, Nilsson F, Reale M. Modulus of elasticity of Norway spruce saw logs vs. structural lumber grade. Holz Als Roh-Und Werkstoff 2006;64(4):273–9.
[2] Fischer C, Vestøl GI, Øvrum A, Høibø OA. Pre-sorting of Norway spruce structural timber using acoustic measurements combined with site, tree and log characteristics. Eur J Wood Wood Prod 2015;73(6):819–28.
[3] Farrell R, Nolan G. Sorting plantation Eucalyptus nitens logs with acoustic wave velocity. Victoria, Australia: Forest & Wood Products Australia Limited; 2008. Project No.PN07.3018.
[4] Koca G, Dündar T, As N. Using the ultrasonic stress wave technique to evaluate structural timber members of an old masonry building. Kastamonu Univ J For 2018;18(3):341–9.
[5] Xu F, Wang XP, Thomas E, Liu YF, Brashaw BK, Ross RJ. Defect detection and quality assessment of hardwood logs: part 1-acoustic impact test and wavelet analysis. Wood Fiber Sci 2018;50(3):291–309.
[6] Xu F, Liu YF, Wang XP, Brashaw BK, Yeary LA, Ross RJ. Assessing internal soundness of hardwood logs through acoustic impact test and waveform analysis. Wood Sci Technol 2019;53(5):1111–34.
[7] Xu F, Liu YF, Wang XP, Brashaw BK, Yeary LA, Ross RJ. Evaluating internal condition of hardwood logs based on AR-minimum entropy deconvolution combined with wavelet based spectral kurtosis approach. Holzforschung 2021;75(3):237–49.
[8] Trnka J, Buchar J, Stoklasová P, Nedomová Š. Response of wood bars to non-destructive impact. Exp Tech 2016;40(5):1387–95.
[9] Lawday G, Hodges PA. The analytical use of stress waves for the detection of decay in standing trees. Forestry 2000;73(5):447–56.
[10] Xu F, Wang X, Teder M, Liu Y. Acoustic impact testing and waveform analysis for damage detection in glued laminated timber. Holzforschung 2017;71(10):801–11.

[11] Zhu X, Liu Y. Detection and location of defects in laminated veneer lumber by wavelet package analysis. Bioresources 2014;9(3):4834–43.
[12] Yu Y, Subhani M, Dackermann U, Li J. Novel hybrid method based on advanced signal processing and soft computing techniques for condition assessment of timber utility poles. J Aerospace Eng 2019;32(4). 04019032.1-04019032.13.
[13] Bandara S, Rajeev P, Gad E, Sriskantharajah B, Flatley I. Damage detection of in service timber poles using Hilbert-Huang transform. NDT Int 2019;107(3). 102141.1-102141.15.
[14] Dragomiretskiy K, Zosso D. Variational mode decomposition. IEEE Trans Signal Process 2014;62(3):531–44.
[15] Diao X, Jiang JC, Shen GD, Chi ZZ, Wang ZR, Ni L, Mebarki A, Bian HT, Hao YM. An improved variational mode decomposition method based on particle swarm optimization for leak detection of liquid pipelines. Mech Syst Signal Process 2020:143.
[16] Hao Y, Du Z, Jiang J, Xing Z, Yan X, Wang S, Rao Y. Research on multipoint leak location of gas pipeline based on variational mode decomposition and relative entropy. Shock Vib 2020;2020(2):1–11.
[17] Saini M, Payal Satija U. An effective and robust framework for ocular artifact removal from single-channel EEG signal based on variational mode decomposition. IEEE Sensor J 2020;20(1):369–76.
[18] Mousavi M, Holloway D, Olivier JC, Gandomi AH. Beam damage detection using synchronisation of peaks in instantaneous frequency and amplitude of vibration data. Measurement 2020;168(1):108297.
[19] Wang XB, Yang ZX, Yan XA. Novel particle swarm optimization-based variational mode decomposition method for the fault diagnosis of complex rotating machinery. IEEE-ASME T Mech 2018;23(1):68–79.
[20] Zhang X, Miao Q, Zhang H, Wang L. A parameter-adaptive VMD method based on grasshopper optimization algorithm to analyze vibration signals from rotating machinery. Mech Syst Signal Process 2018;108:58–72.
[21] Li HX, Chang JH, Xu F, Liu ZX, Yang ZB, Zhang LY, Zhang SY, Mao RX, Dou XL, Liu BG. Efficient Lidar signal denoising algorithm using variational mode decomposition combined with a whale optimization algorithm. Rem Sens 2019;11(2):126.
[22] Song EZ, Ke Y, Yao C, Dong Q, Yang LP. Fault diagnosis method for high-pressure common rail injector based on IFOA-VMD and hierarchical dispersion entropy. Entropy 2019;21(10):923.
[23] Xu B, Zhou FX, Li HP, Yan BK, Liu Y. Early fault feature extraction of bearings based on Teager energy operator and optimal VMD. ISA Trans 2019;86:249–65.
[24] Zhu J, Wang C, Hu ZY, Kong FR, Liu XC. Adaptive variational mode decomposition based on artificial fish swarm algorithm for fault diagnosis of rolling bearings. P I Mech Eng C- J Mec 2017;231(4):635–54.
[25] Kennedy J, Eberhart R. Particle swarm optimization. In: Proceedings of the IEEE international conference on neural networks, Perth, Australia, vol. 4; 1995. p. 1942–8.
[26] Kennedy J. Particle swarm optimization in encyclopedia of machine learning. Boston, MA, USA: Springer; 2011. p. 760–6.
[27] Dackermann U, Crews K, Kasal B, Li J, Riggio M, Rinn F, Tannert T. In situ assessment of structural timber using stress-wave measurements. Mater Struct 2014;47(5):787–803.
[28] Dunlop JI. Testing of poles by acoustic resonance. Wood Sci Technol 1983;17(1):31–8.
[29] Mucciardi AN, Luley CJ, Gormally KH. Preliminary evidence for using statistical classification of vibration waveforms as an initial decay detection tool. Arboric Urban For 2011;37(5):191–9.
[30] Hsiao C, Cheng CC, Liou T, Juang Y. Detecting flaws in concrete blocks using the impact-echo method. NDT Int 2008;41(2):98–107.